

---

# Leveraging Perfect Multimodal Alignment and Gaussian Assumptions for Cross-modal Transfer

---

**Abhi Kamboj**

Electrical and Computer Engineering  
University of Illinois  
akamboj2@illinois.edu

**Minh N. Do**

Electrical and Computer Engineering  
University of Illinois  
minhdo@illinois.edu

## Abstract

Multimodal alignment aims to construct a joint latent vector space where two modalities representing the same concept map to the same vector. We formulate this as an inverse problem and show that under certain conditions perfect alignment can be achieved. We then address a specific application of alignment referred to as cross-modal transfer. Unsupervised cross-modal transfer aims to leverage a model trained with one modality to perform inference on another modality, without any labeled fine-tuning on the new modality. Assuming that semantic classes are represented as a mixture of Gaussians in the latent space, we show how cross-modal transfer can be performed by projecting the data points from the representation space on to difference subspaces representing each modality. Our experiments on synthetic multimodal Gaussian data verify the effectiveness of our perfect alignment and cross-modal transfer method. We hope these findings inspire further exploration of the applications of perfect alignment and the use of Gaussian models for cross-modal learning.

## 1 Introduction

Humans are naturally able to perceive the same concept through multiple senses. Artificial intelligence attempts to mimic this with multimodal data. Multimodal data can be leveraged jointly through one large model trained with all the modalities and tested with all the modalities. However, this method is limited given the differences in modalities. For example, some modalities are very abundant, such as images and text from the internet, whereas others are less abundant, such as MRI or ECG data. Some modalities are more detailed and information rich such as images whereas others are more privacy preserving such as mmwRadar or IMU. Some modalities are easy to annotate such as video, whereas others are more difficult such as EMG data. So how can we leverage the modalities that are abundant, easy to annotate and easy to learn more to perform better with the more difficult modalities?

An alternative, more flexible approach involves a model that can learn to leverage multiple modalities separately by learning relations among them. More specifically, in order to understand multimodal data, AI methods perform alignment between the semantic meanings of the data. For example, an AI model can associate an image with text describing that image Radford et al. [2021], or sounds that things in that image might make Girdhar et al. [2023]. However, these learned alignment methods are approximate, and lack theoretical rigour and interpretability.

Past works have attempted to understand alignment through geometric Wang and Isola [2020], probabilistic Chen et al. [2024], Che and Eysenbach [2025], and information-theoretic Oord et al. [2018], Poole et al. [2019] interpretations. In this work we model contrastive alignment as an inverse problem in vector signal processing to recover a representation space with perfect alignment across two modalities. Perfect alignment implies that we can construct encoders  $f^1$  and  $f^2$  for modalities 1

and 2 respectively, such that for every data instance seen during training  $f^1$  and  $f^2$  map that instance from the data of each modality to the same latent representation  $z$ .

Using this perfect reconstruction, we formulate a method to perform unsupervised cross modality transfer. Unsupervised cross-modal transfer aims to leverage a model trained with one modality to perform inference on another modality, without any labeled fine tuning on the new modality. This can be done by performing unsupervised multimodal representation learning across the modalities. Assuming that the representation space is modeled as a mixture of multivariate Gaussian and different modalities are generated as a projection from this latent space, we show how semantic information can be transferred across the representation space through cross-modal projections. The key property that a linear projection of a Gaussian distribution is still gaussian allows us to perform this transfer. Furthermore, the perfect alignment between the modalities that we were able to recover through our inverse problem formulation allows for a theoretically maximal few-shot cross-modal transfer performance. Our full process is depicted in Figure 1. We test our methods on synthetic data and real-world data align and show competitive performance compared to typical contrastive learning based gradient descent. We believe these results indicate a far reaching potential of Gaussian data to be used to model every day interpretations of our world (projections of the latent space to modalities) and hope this inspires further investigation of multimodal Gaussian data.

We also provide some insight into the platonic representation hypothesis that argues representations from different modalities are converging Huh et al. [2024]. Our method and results neither support or denies this but brings about a related conclusion that their exists, and it can be computed, some perfect alignment space between two modalities that are perfect in the empirical sense in that they can model only the data they have seen in perfect alignment. This leaves room for interested researchers to leverage such a perfect alignment for tasks such as zeroshot classification, cross modal retrieval, cross-modal transfer, cross modal generation and many other applications tasks. Our work offers insights into the platonic representation hypothesis, which posits that representations of the same semantic concepts from different modalities converge to the same latent representation space Huh et al. [2024]. While our method and results neither fully confirm nor refute this hypothesis, they suggest the existence of a perfect alignment space between two modalities, empirically demonstrated by their ability to model seen data in perfect alignment. This finding opens opportunities for researchers to leverage such alignment in tasks like zero-shot classification, cross-modal retrieval, transfer, generation, and other applications.

## 2 Methods

### 2.1 Perfect Multimodal Alignment

In the following section we propose a method to perform perfect alignment between various modalities. In our notation we assume a superscript indicates a different modality, a subscript indicates a different data point, a lowercase letter indicates a column vector, and capital letter indicates a matrix, and a calligraphic capital letter indicates a vector space unless otherwise specified. Our notation is indexed starting at 1.

Also, note that in our formulation we avoid using the phrase multimodal gaussian which in the literature often refers to a mixture of gaussians that have different modes. This is so we do not confuse the modes of a gaussian with the modalities which our gaussian represents. In reality, we formulate the modes (or peaks) of the gaussian as different classes, as typically is done with Gaussian mixture models), and we argue the features from each modality can be represented by a subspace in  $\mathcal{Z}$ .

Suppose we have some ground truth latent space  $\mathcal{Z} \subseteq \mathbb{R}^k$  representing various concepts. We assume each modality  $m$  is generated by some transformation over this latent space  $S^m$ , e.g. a given data point  $i$ ,  $x_i^{(m)} = S^{(m)} z_i$ . Thus the data for two modalities of the same sample  $i$  is given by  $x_i^{(1)} = S^{(1)} z_i$  and  $x_i^{(2)} = S^{(2)} z_i$  where  $x_i^{(1)} \in \mathcal{X}^1 \subseteq \mathbb{R}^{d_1}$ ,  $S^{(1)} \in \mathbb{R}^{d_1 \times k}$  and  $x_i^{(2)} \in \mathcal{X}^{(2)} \subseteq \mathbb{R}^{d_2}$ ,  $S^{(2)} \in \mathbb{R}^{d_2 \times k}$ . Now we aim to recover the vector  $z_i$  which generated these modalities, e.g. we approximate  $S^{(1)-1}$  and  $S^{(2)-1}$  using  $A^{(1)}$  and  $A^{(2)}$  such that  $A^{(1)} x_i^{(1)} = A^{(2)} x_i^{(2)} = z_i$  for all  $i$  in a given dataset. Note that we assume we do not have access to  $S^{(1)}$  and  $S^{(2)}$ , as these were some transformations that

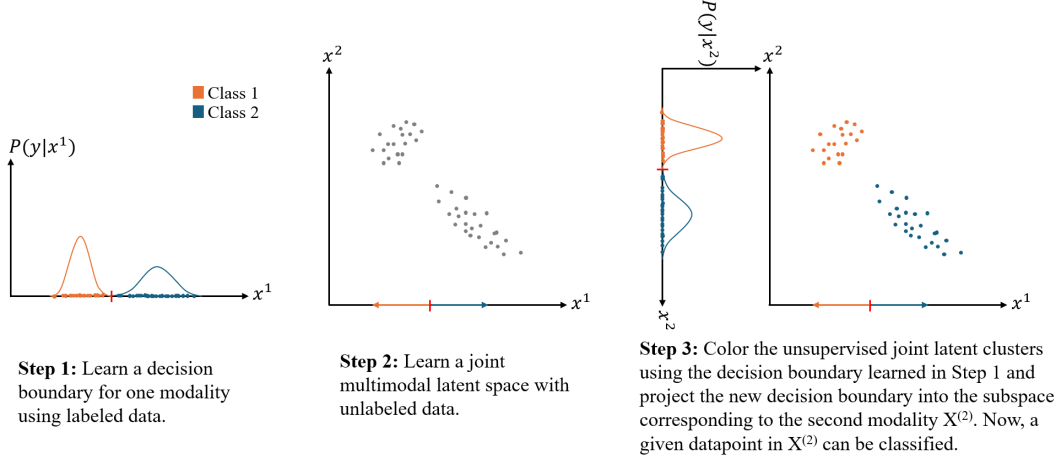


Figure 1: This figure depicts the process of performing unsupervised cross-modality transfer, in the simple case where the relevant features from each modality ( $x^1$  and  $x^2$ ) is the 1-dimensional subspace spanned by each principle axis, however, we believe it generalizes to any dimensional sized vectors and subspaces. Furthermore, the semantic classes in the representation space can be modeled as a mixture of multivariate gaussians. Step 1 involves learning the distribution  $P(y|x^1)$  given a set of labeled data points from the first modality  $\{(x^1, y)\}_{i=1}^N$ , and determining a decision boundary, depicted as a red line. Step 2, learns a joint multimodal latent space by clustering together representations constructed by concatenating the data vectors from both modalities. Step 3 labels those clusters based on the decision boundary determined in Step 1, and infers a decision boundary for datapoints in the second modality ( $x^2$ ).

generated our naturally occurring data  $X^{(1)}$  and  $X^{(2)}$  from the same concept. Figure 2 illustrates this model.

Rewritten we have to solve:

$$A^{(1)}x_i^{(1)} - A^{(2)}x_i^{(2)} = 0, \forall i = 1 \dots n. \quad (1)$$

Assume we stack all  $n$  data points as column vectors horizontally, we have  $X^{(1)} = [x_1^{(1)}, x_2^{(1)} \dots x_n^{(1)}] \in \mathbb{R}^{d_1 \times n}$  and  $X^{(2)} = [x_1^{(2)}, x_2^{(2)} \dots x_n^{(2)}] \in \mathbb{R}^{d_2 \times n}$ . Furthermore, we can stack  $A^{(1)}$  and  $A^{(2)}$  horizontally as  $A = [A^{(1)} | A^{(2)}] \in \mathbb{R}^{k \times d}$  and stack  $X^{(1)}$  and  $X^{(2)}$  vertically as  $X = \begin{bmatrix} X^{(1)} \\ X^{(2)} \end{bmatrix} \in \mathbb{R}^{d \times n}$  where  $d = d_1 + d_2$ .

Thus Equation (1) becomes the following inverse problem:

$$AX = \mathbf{0} \quad (2)$$

where  $\mathbf{0} \in \mathbb{R}^{k \times n}$  is a matrix of zeros,  $X$  is given and we must solve for  $A$  such that  $A$  is nonzero.

**Theorem 2.1** (Existence of Perfect Alignment). *Given the inverse problem  $AX = \mathbf{0}$  constructed in Equation (2), where  $X \in \mathbb{R}^{d \times n}$  is a given matrix and  $A \in \mathbb{R}^{k \times d}$  is unknown, if  $X$  has a null space of at least  $k$  dimensions, then there exists a closed-form solution for  $A$ . Specifically, the rows of  $A$  can be formed by any  $k$  vectors that constitute a basis for the left null space of  $X$ .*

*Proof.* The proof involves recognizing that any vector  $a$  in the left null space of  $X$  satisfies  $a^T X = 0$ . Therefore, if  $X$  has a null space of dimension at least  $k$ , we can select  $k$  linearly independent vectors from this null space to form the rows of  $A$ . This ensures that  $AX = 0$  is satisfied.  $\square$

**Corollary 2.2** (Approximate Alignment). *Even if  $X$  is a full column rank matrix, or has a null space with less than  $k$  dimensions, an approximation of the solution to  $AX = 0$  can be obtained considering the basis vectors corresponding to the smallest singular values of  $X$ . These vectors are the least representative of the principal components of  $X$  and can be used to construct an approximate solution for  $A$ .*

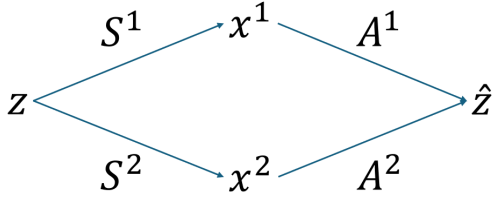


Figure 2: **Data Generation Pipeline:** Some latent concept vector  $z$  generates data that occurs in nature and is read through various modalities  $x^{(1)}$  and  $x^{(2)}$  through transformations  $S^{(1)}$  and  $S^{(2)}$ . We attempt to approximate  $z$  by determining projections  $A^{(1)}$  and  $A^{(2)}$ .

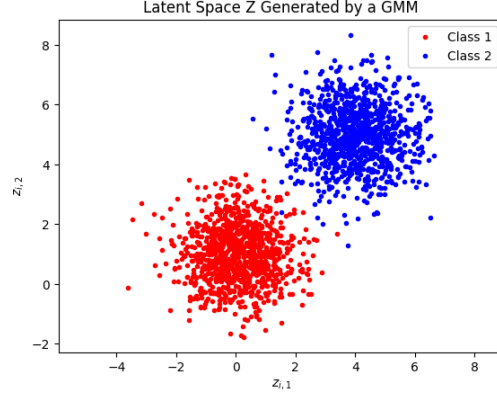


Figure 3: **Generated Latent Space:** This shows the generated 2-dimensional mixture of two gaussian latent space generated for our synthetic experiments as described in Section 3.

**Method for Finding  $A$ :** To determine  $A$ , perform the Singular Value Decomposition (SVD) of  $X$ , yielding  $X = U\Sigma V^T$ . Then, extract the last  $k$  columns of  $U$ , denoted as  $u_{d-(k-1)}, \dots, u_{d-1}, u_d$ , where  $U \in \mathbb{R}^{d \times d}$  and  $k < d$ . The last  $k$  columns of  $U$  correspond to the basis vectors of the left null space of  $X$  when its dimension is at least  $k$ . For matrices  $X$  with a smaller left null space, these vectors correspond to the lowest signal components (lowest singular values) and provide an approximation of the solution in the minimum frobenius norm sense. The solution for  $A$  can be expressed as:

$$A^* = [u_{d-(k-1)} \dots u_{d-1}, u_d] \quad (3)$$

where  $u_j$  represents the  $j^{\text{th}}$  column of  $U$ . This method is both a solution for the perfect alignment when the null space is sufficiently large and an approximation otherwise.

*Remark 2.3* (Assumption on  $k$  and  $d$ ). The assumption that  $k < d$  is valid because, in many machine learning applications, the dimension of the latent or feature space ( $k$ ) is typically less than the dimension of the data ( $d$ ). This is a common scenario in representation learning, where the goal is to represent high-dimensional data in a lower-dimensional space while preserving essential information.

*Remark 2.4* (Achievability and Computational Cost of Perfect Alignment). In machine learning, perfect alignment can often be achieved because the number of data points  $n$  is typically large. This allows for a sufficiently large left null space in  $X$ , enabling the computation of  $A$  such that  $AX = 0$ . However, computing  $A$  via SVD of  $X$  (a  $d \times n$  matrix) can be computationally expensive. The full SVD has a large time complexity of  $O(d^2n + dn^2 + n^3)$ , which explains why approximate methods such as gradient descent are dominant in machine learning.

## 2.2 Error Metrics for Perfect Alignment

Next we establish two error metrics to determine how good of an estimation  $A^*$  is. The first sense of error we care about is how well the  $z$  reconstructed from both modalities align. Let  $\hat{z}^1 = A^1 x^1$  and  $\hat{z}^2 = A^2 x^2$  then the alignment error is given as follows:

$$\text{Error Alignment} = \frac{1}{n} \sum_{i=1}^n \|\hat{z}_i^1 - \hat{z}_i^2\| \quad (4)$$

where  $n$  is the datapoints for which the alignment error is being computed for. Furthermore, we care about a reconstruction error which identifies how well each modality estimation approximates the correct  $z$ . This reconstruction is given by:

$$\text{Error Reconstruction for } S^m = \frac{1}{n} \sum_{i=1}^n \|z_i - \hat{z}_i^m\| \quad (5)$$

Error Metric	Value
Average Reconstruction Error $S^{(1)}$	10.9271
Average Reconstruction Error $S^{(2)}$	10.9271
Average Alignment Error	$3.66 \times 10^{-15}$
Average Reconstruction Error using $S^{(1)\dagger}$	$2.98 \times 10^{-16}$
Average Reconstruction Error using $S^{(2)\dagger}$	$6.47 \times 10^{-16}$

Figure 4: Reconstruction and Alignment Errors.  $\dagger$  denotes pseudo-inverse.

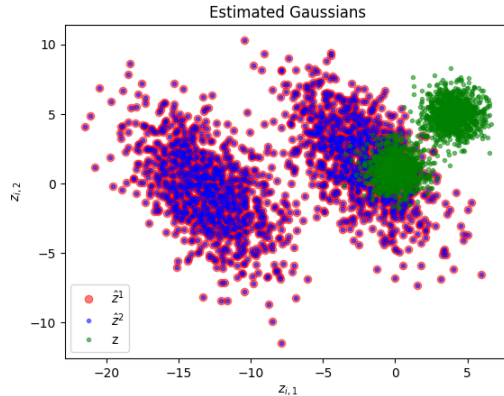


Figure 5: **Estimated Latent Space:** This shows the estimated latent space recovered from our alignment technique on our synthetic data experiments as described in Section 3.

We note that the alignment error is always applicable, however, the reconstruction error can only be computed in toy experiments, as with real data the true concept vector  $z$  is unknown.

### 3 Experiments

#### 3.1 Synthetic Data

**Data Generation:** We generate the data from a synthetic ground truth latent space  $Z$  which is constructed as a mixture of two two-dimensional Gaussian distributions.

$$Z \sim \pi_1 \mathcal{N}(\mu_1, \Sigma_1) + \pi_2 \mathcal{N}(\mu_2, \Sigma_2), \text{ where } \pi_1 = \pi_2 = .5, \mu_1, \mu_2 \in \mathbb{R}^2, \Sigma_1, \Sigma_2 \in \mathbb{R}^{2 \times 2}. \quad (6)$$

We manually  $\mu_1 = [0, 1]^T$  and  $\mu_2 = [4, 5]^T$  and set  $\Sigma_1$  and  $\Sigma_2$  to be the 2-dimensional identity matrix for visual simplicity. First, we sample 2000 vectors from  $Z$ ,  $\mathcal{D}_Z = \{z_i\}_{i=1}^{2000}$  and then project them into modalities 1 and 2 using randomly determined  $2 \times 2$  matrices  $S^{(1)}$  and  $S^{(2)}$ , with values ranging from -5 to 5, i.e.

$$\mathcal{D}_{x^{(1)}} = \{x_i^{(1)} = S^{(1)} z_i\}_{i=1}^{2000}, \mathcal{D}_{x^{(2)}} = \{x_i^{(2)} = S^{(2)} z_i\}_{i=1}^{2000} \quad (7)$$

The data generation pipeline can be visualized in Figure 2 and the generated latent space is shown in Figure 3.

#### Alignment and Reconstruction Errors:

We determine  $A$  using the method outlined in Section 2.1 and compute the average alignment and reconstruction errors as specified in Section 2.2. These results are presented in Figure 4, and a visualization is shown on in Figure 5.

The initial results indicate that the alignment error is typically very low with our proposed solver, whereas the reconstruction error is high. The visualization further shows that the  $\hat{z}^1$  and  $\hat{z}^2$  points overlap almost precisely however they form different clusters from the original GMM. This outcome is consistent with the fact that the solution to Equation (2) is non-unique. Specifically, the basis formed by the columns in Equation (3) can be arbitrarily linearly scaled to produce another valid solution. We hypothesize that one of these solutions might achieve both perfect reconstruction and alignment, but this poses a more challenging optimization problem.

Interestingly, although the clusters formed are different the transformation preserves the clusters as a linear transformation of gaussian is still gaussian. This implies that classes can still be determined in this estimated latent space even if we don't recover the exact original space.

Notably, despite the differences in the formed clusters, the transformation preserves their structure. This is because a linear transformation of a Gaussian distribution remains Gaussian. Consequently,

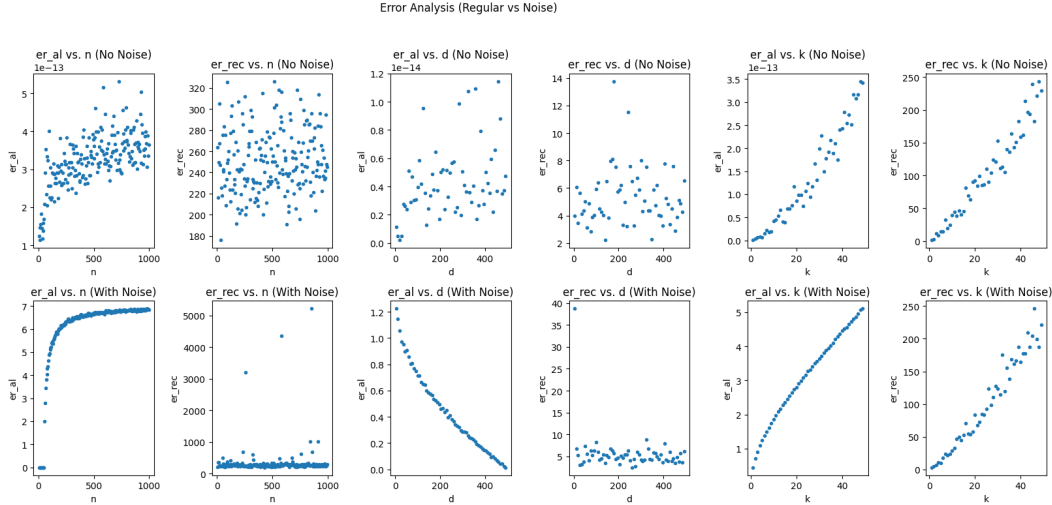


Figure 6: **Vary the Parameters and Adding noise:** This shows the calculated errors when using our solvers on various parameters. In the first two columns we change the number of datapoints  $n$ . In the second two columns we change the dimension of the data  $d$ . In the third two columns we change the hidden latent vector dimension  $k$ . The first row shows the results without noise, the second row shows the results when the generated data has standard gaussian noise added to it.

the classes can still be identified in the estimated latent space using a GMM, even if the exact original space is not recovered.

#### 4 Conclusion:

In this paper, we proposed a method for achieving perfect multimodal alignment by solving an inverse problem that projects data from different modalities onto a shared latent space. Our approach involves determining matrices  $A^{(1)}$  and  $A^{(2)}$  such that  $A^{(1)}x^{(1)} = A^{(2)}x^{(2)}$  for all data points, effectively aligning the modalities. We demonstrated that this method can achieve low alignment errors in synthetic experiments, although reconstruction errors remain high due to the non-uniqueness of the solution. Notably, the transformation preserves the Gaussian structure of the data, allowing for class identification in the estimated latent space even if the original space is not exactly recovered. Our findings highlight the potential of this alignment technique for multimodal data analysis and suggest avenues for future research in optimizing reconstruction errors and applying this method to real-world datasets.

#### References

- Yongwei Che and Benjamin Eysenbach. The "law" of the unconscious contrastive learner: Probabilistic alignment of unpaired modalities. *arXiv preprint arXiv:2501.11326*, 2025.
- Zihao Chen, Chi-Heng Lin, Ran Liu, Jingyun Xiao, and Eva Dyer. Your contrastive learning problem is secretly a distribution alignment problem. *Advances in Neural Information Processing Systems*, 37:91597–91617, 2024.
- Rohit Girdhar, Alaeldin El-Nouby, Zhuang Liu, Mannat Singh, Kalyan Vasudev Alwala, Armand Joulin, and Ishan Misra. Imagebind: One embedding space to bind them all. In *Proceedings of the IEEE/CVF Conference on Computer Vision and Pattern Recognition (CVPR)*, pages 15180–15190, June 2023.
- Minyoung Huh, Brian Cheung, Tongzhou Wang, and Phillip Isola. Position: The platonic representation hypothesis. In *Proceedings of the 41st International Conference on Machine Learning*, volume 235 of *Proceedings of Machine Learning Research*, pages 20617–20642. PMLR, 2024. URL <https://proceedings.mlr.press/v235/huh24a.html>.

- Aaron van den Oord, Yazhe Li, and Oriol Vinyals. Representation learning with contrastive predictive coding. *arXiv preprint arXiv:1807.03748*, 2018.
- Ben Poole, Sherjil Ozair, Aaron Van Den Oord, Alex Alemi, and George Tucker. On variational bounds of mutual information. In *International conference on machine learning*, pages 5171–5180. PMLR, 2019.
- Alec Radford, Jong Wook Kim, Chris Hallacy, Aditya Ramesh, Gabriel Goh, Sandhini Agarwal, Girish Sastry, Amanda Askell, Pamela Mishkin, Jack Clark, Gretchen Krueger, and Ilya Sutskever. Learning transferable visual models from natural language supervision. In Marina Meila and Tong Zhang, editors, *Proceedings of the 38th International Conference on Machine Learning*, volume 139 of *Proceedings of Machine Learning Research*, pages 8748–8763. PMLR, 18–24 Jul 2021. URL <https://proceedings.mlr.press/v139/radford21a.html>.
- Tongzhou Wang and Phillip Isola. Understanding contrastive representation learning through alignment and uniformity on the hypersphere. In *International conference on machine learning*, pages 9929–9939. PMLR, 2020.